Electrically Tunable Polypyrrole Inverse Opals with Switchable Stopband, Conductivity, and Wettability

Liang Xu,[†] Jingxia Wang,*[,‡] Yanlin Song,*[,†,‡] and Lei Jiang[†]

Beijing National Laboratory for Molecular Sciences (BNLMS) Key Laboratory of Organic Solids and The Laboratory of New Materials, Institute of Chemistry, Chinese Academy of Sciences, Beijing 100080, P. R. China

Received February 13, 2008
Revised Manuscript Received April 18, 2008

Photonic crystals[1] (PCs) have aroused extensive attention due to their special light manipulating properties and showed potential applications in smart windows, chemical sensors, optical devices, and memory devices.[2–8] Recently, a growing research interest has been focused on the fabrication of multifunctional PCs.[9] For example, Sailor et al.[9a] reported an amphiphilic, magnetic bifunctional PC, which could manipulate liquid droplets without microfluidic container, and its structure color provided an optical signal to distinguish different liquids. These multifunctional PCs demonstrated extra properties except stopband of PCs and greatly extended their promising applications. Herein, a new multifunctional PC was fabricated based on the polypyrrole (Ppy) material.

Ppy is an electrically active material, whose properties can be reversibly modulated by doping or dedoping different ions,[10] offering it many potential applications in various devices.[10–13] Typically, based on its large volume change between reduction and oxidation state, Ppy has been used as microactuators.[11] Meanwhile, a microfluidic device can be achieved based on its switchable wettability from superhydrophobicity to superhydrophilicity by controlling electrochemical potential,[12] while the fabrication of Ppy PCs would endow them novel optical properties.[13] Caruso et al. have successfully developed Ppy inverse opals for biosensing[13b,c] and fluorescence control.[13d] However, the reversible tuning of Ppy properties has not be reported in the Ppy PC, which would be of great importance for applications in smart optoelectronic devices. In this paper, the Ppy inverse opal with switchable stopband, conductivtiy, and wettability was successfully fabricated using high-quality PC template made from latex spheres with hydrophobic PS core and hydrophilic PMMA-PAA shell. These properties endow the Ppy inverse opal promising application in novel multifunctional optical devices.

The PC templates were prepared via vertical depositon from the core−shell latex suspension of poly(St-MMA-AA) with a diameter of ca. 440 nm. Here, the specific dimension of latex spheres ensured that the stopband of the Ppy inverse opal located in the visible range under different doping levels. Meanwhile, this latex diameter provided enough air interstice for easily filling of the pyrrole monomer. Moreover, the specific morphology of the latex spheres, with hydrophobic PSt core and hydrophilic PMMA-PAA shell,[14] was favorable to the permeation of pyrrole aqueous solution into the opal void due to the hydrogen bonding interaction between the amide and the carboxyl groups. Additionally, the strong hydrogen bonding between the hydrophilic latex shell and hydrophilic ITO substrate could prevent the PC structure from being damaging when the film was exposed to aqueous electrolyte. Figure 1a,b shows typical top and cross views of SEM images of the PC templates. The images showed that the latex particles were face-centered cubic close-packed, with the (111) surface parallel to the ITO substrate. This

* Corresponding author. E-mail: wangzhang@iccas.ac.cn, ylsong@iccas.ac.cn.
[†] Beijing National Laboratory for Molecular Sciences (BNLMS) Key Laboratory of Organic Solids.
[‡] The Laboratory of New Materials.

(1) (a) Yablonovitch, E. *Phys. Rev. Lett.* **1987**, *58*, 2059. (b) John, S. *Phys. Rev. Lett.* **1987**, *58*, 2486.
(2) (a) Gu, Z-Z.; Fujishima, A.; Sato, O. *J. Am. Chem. Soc.* **2000**, *122*, 12387. (b) Kubo, S.; Gu, Z-Z.; Takahashi, K.; Ohko, Y.; Sato, O.; Fujishima, A. *J. Am. Chem. Soc.* **2002**, *124*, 10950. (c) Kumoda, M.; Watanabe, M.; Takeoka, Y. *Langmuir* **2006**, *22*, 4403.
(3) (a) Ozaki, M.; Shimoda, Y.; Kasano, M.; Yoshino, K. *Adv. Mater.* **2002**, *14*, 514. (b) Xia, J.; Ying, Y.; Foulger, S. H. *Adv. Mater.* **2005**, *17*, 2463. (c) Norton, J. C. S.; Han, M. G.; Jiang, P.; Shim, G. H.; Ying, Y. R.; Creager, S.; Foulger, S. H. *Chem. Mater.* **2006**, *18*, 457.
(4) (a) Xu, X.; Friedman, G.; Humfeld, K. D.; Majetich, S. A.; Asher, S. A. *Adv. Mater.* **2001**, *13*, 1681. (b) Xu, X.; Majetich, S. A.; Asher, S. A. *J. Am. Chem. Soc.* **2002**, *124*, 13864. (c) Ge, J.; Hu, Y.; Yin, Y. *Angew. Chem., Int. Ed.* **2007**, *46*, 7428.
(5) (a) Foulger, S. H.; Jiang, P.; Lattam, A. C.; Smith, D. W.; Ballato, J.; Dausch, D. E.; Grego, S.; Stoner, B. R. *Adv. Mater.* **2003**, *15*, 685. (b) Takeoka, Y.; Watanabe, M. *Adv. Mater.* **2003**, *15*, 199. (c) Reese, C. E.; Mikhonin, A. V.; Kamenjicki, M.; Tikhonov, A.; Asher, S. A. *J. Am. Chem. Soc.* **2004**, *126*, 1493. (d) Matsubara, K.; Watanabe, M.; Takeoka, Y. *Angew. Chem., Int. Ed.* **2007**, *46*, 1688.
(6) (a) Foulger, S. H.; Jiang, P.; Lattam, A. C.; Smith, D. W.; Ballato, J. *Langmuir* **2001**, *17*, 6023. (b) Lee, Y. J.; Braun, P. V. *Adv. Mater.* **2003**, *15*, 563.
(7) (a) Ueno, K.; Matsubara, K.; Watanabe, M.; Takeoka, Y. *Adv. Mater.* **2007**, *19*, 2807. (b) Arsenault, A. C.; Puzzo, D. P.; Manners, I.; Ozin, G. A. *Nat. Photon.* **2007**, *1*, 468.
(8) (a) Fudouzi, H.; Xia, Y. *Adv. Mater.* **2003**, *15*, 892. (b) Holtz, J. H.; Asher, S. A. *Nature* **1997**, *389*, 829. (c) Arsenault, A. C.; Miguez, H.; Kitaev, V.; Ozin, G. A.; Manners, I. *Adv. Mater.* **2003**, *15*, 503.
(9) (a) Dorvee, J. R.; Derfus, A.; Bhatia, S. N.; Sailor, M. J. *Nat. Mater.* **2004**, *3*, 896. (b) Brozell, A. M.; Muha, M. A.; Abed-Amoli, A.; Bricarello, D.; Parikh, A. N. *Nano Lett.* **2007**, *7*, 3822. (c) Park, J. H.; Derfus, A. M.; Segal, E.; Vecchio, K. S.; Bhatia, S. N.; Sailor, M. J. *J. Am. Chem. Soc.* **2006**, *128*, 7938. (d) Orosco, M. M.; Pacholski, C.; Miskelly, G. M.; Sailor, M. J. *Adv. Mater.* **2006**, *18*, 1393.
(10) (a) Li, Y.; Qian, R. *J. Electro. Chem.* **1993**, *362*, 267. (b) Li, Y. *Electrochim. Acta* **1997**, *42*, 203. (c) Tezuka, Y.; Ohyama, S.; Ishii, T.; Aoki, K. *Bull. Chem. Soc. Jpn.* **1991**, *64*, 2045. (d) Bredas, J. L.; Street, G. B. *Acc. Chem. Res.* **1985**, *18*, 309. (e) Murray, P.; Spinks, G. M.; Wallace, G. G.; Burford, R. P. *Synth. Met.* **1997**, *84*, 847.
(11) (a) Smela, E.; Gadegaard, N. *Adv. Mater.* **1999**, *11*, 953. (b) Jager, E. W. H.; Smela, E.; Ingana, O. *Science.* **2000**, *290*, 1540. (c) Smela, E. *Adv. Mater.* **2003**, *15*, 481.
(12) Xu, L.; Chen, W.; Mulchandani, A.; Yan, Y. *Angew. Chem., Int. Ed.* **2005**, *44*, 6009.
(13) (a) Sumida, T.; Wada, Y.; Kitamura, T.; Yanagida, S. *Chem. Commun.* **2000**, 1613. (b) Cassagneau, T.; Caruso, F. *Adv. Mater.* **2002**, *14*, 34–1837. (c) Cassagneau, T.; Caruso, F. *Adv. Mater.* **2002**, *14*, 1837. (d) Yu, A.; Meiser, F.; Cassagneau, T.; Caruso, F. *Nano Lett.* **2004**, *4*, 177. (e) Cho, G.; Jung, M.; Yang, H.; Lee, B.; Song, J. H. *Mater. Lett.* **2007**, *61*, 1086. (f) Lee, J.; Lee, D.; Kim, J.; Cheong, I. *Macromolecules* **2007**, *40*, 9529.
(14) (a) Wang, J.; Wen, Y.; Feng, X.; Song, Y.; Jiang, L. *Macromol. Rapid Commun.* **2006**, *207*, 596. (b) Wang, J.; Hu, J.; Wen, Y.; Song, Y.; Jiang, L. *Chem. Mater.* **2006**, *18*, 4984. (c) Wang, J.; Wen, Y.; Hu, J.; Song, Y.; Jiang, L. *Adv. Funct. Mater.* **2007**, *17*, 219. (d) Wang, J.; Wen, Y.; Ge, H.; Song, Y.; Jiang, L. *Macromol. Chem. Phys.* **2006**, *207*, 596. (e) Tian, E.; Wang, J.; Zheng, Y.; Song, Y.; Jiang, L.; Zhu, D. *J. Mater. Chem.* **2008**, *18*, 1116.

10.1021/cm800444a CCC: $40.75
Published on Web 05/07/2008

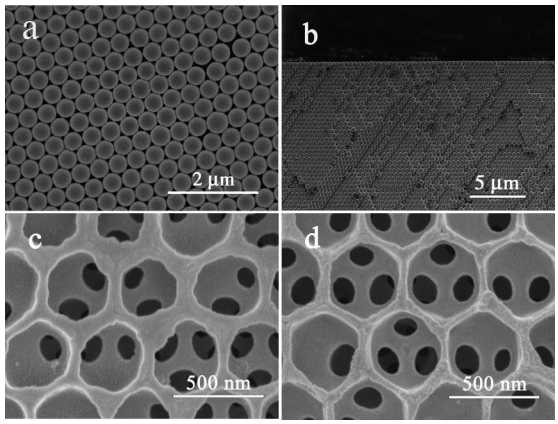

Figure 1. Typical SEM images (a and b) for the PC template, and (c and d) for the oxidation and neutral state of Ppy inverse opals.

Scheme 1

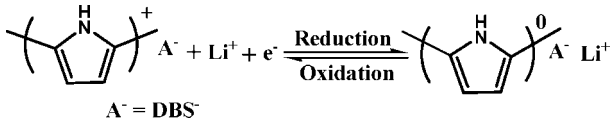

well-ordered PC template was necessary for the formation of high quality Ppy inverse opal.

Ppy inverse opals were prepared by electrodeposition technique.[13] The reaction was carried out in a three electrodes electrochemical cell. The pyrrole (0.1 M) was dissolved in 0.1 M sodium dodecylbenzene sulfonate (NaDBS) aqueous electrolyte to infiltrate into the void of the PC template. Following the electropolymerization, the poly(St-MMA-AA)−Ppy composite opal was exposed to tetrahydrofuran for 24 h to remove the poly(St-MMA-AA) PC template. The as-prepared Ppy inverse opal exhibited green color. Figure 1c and Figure S3 (Supporting Information) showed the SEM images of the freshly prepared Ppy inverse opal. Clearly, the pores were in ordered array, consistent with a (111) plane arrangement of the original latex templates. The center-to-center distance of the resulting inverse opal was 360 ± 20 nm, and the wall thickness was 60 ± 5 nm. The thickness of the film was ca. 2 μm (see Figure S4, Supporting Information).

The properties of the Ppy inverse opal were modulated by electrochemical redox,[10–12] which was carried out in an electrochemical cell filled with 0.1 M aqueous $LiClO_4$ solution. In our systerm, doping or dedoping of the small Li^+ dominated the electrochemical redox due to the large immobile DBS^- as dopant.[10a,c,d,11b] (see Figure S1, Supporting Information). Scheme 1 presents the reaction of electrochemical redox of Ppy, and the dedoping and doping of Li^+ resulted in the change of the film from oxidation to neutual state.

The optical propeties of the Ppy inverse opals can be modified by electrochemical redox. Figure 2a presented the UV−vis spectra of the Ppy inverse opals at oxidation (the green line) and neutral state (the orange one) respectively. The stopband position of the Ppy film at oxidation state was 576 nm, and the value red-shifted to 626 nm at neutral state. Meanwhile, the color of the film changed from green to orange as shown in the inset of Figure 2a. Furthermore, the stopband position could return to 576 nm accompanying with its color change (from orange to green) when being reoxi-

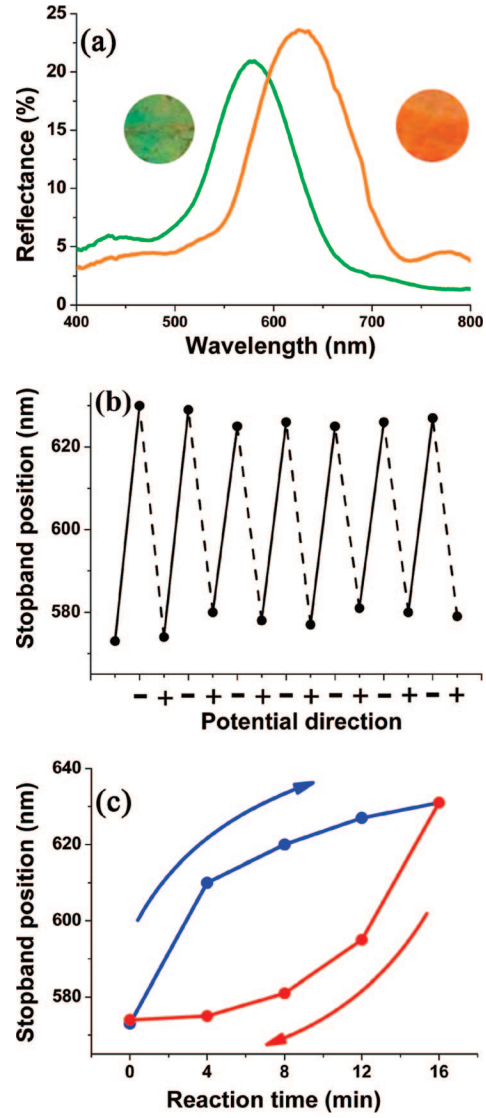

Figure 2. (a) UV−vis spectra of the Ppy inverse opal at the oxidation (the green line) and neutral state (the orange line). The insets were the microscope photographs of the film at the oxidation (green) and neutral (orange) state, respectively. (b) Reversible stopband transitions of the Ppy inverse opal upon alternative negative potential (−0.8 V vs $Hg/HgCl_2$) and positive potential (0.8 V vs $Hg/HgCl_2$), respectively. (c) The relationship of stopband positions and oxidation/reduction times, with the arrows indicating the reaction direction of the electrochemical redox.

dized. Figure 2b presented the reversible change of stopband position when alternatively exposing the film at negative potential (−0.8 V vs $Hg/HgCl_2$) and positive potential (0.8 V vs $Hg/HgCl_2$), respectively. The change of peak positions was steadily reversible though there was a small fluctuation. The samples showed good durability during tens of cyclic experiments, which would be of great importance for practical application for optoelectronic or sensor devices.

The stopband of the Ppy inverse opal was determined by the lattice constant and the refractive index.[15a] In our system, the change of the stopband was mainly resulted from doping and dedoping of Li^+, which led to the increae/decrease of both volume and refractive index of Ppy.[11,13d,e,15b] The volume increase could be clearly observed when comparing the SEM image of the Ppy inverse opal at the oxidation (Figure 1c) with that at the neutral state (Figure 1d). Obviously, the average size of the sphere voids increased by 30−50 nm, and the wall thickness thinned by 20 nm when the film varied from oxidation

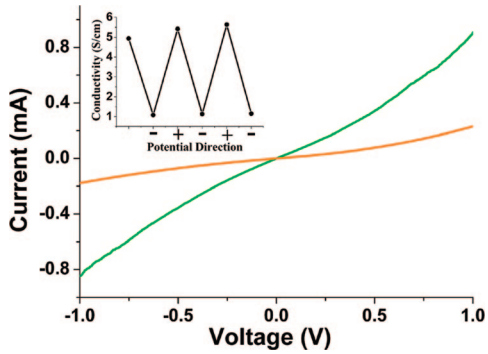

Figure 3. *I/V* curve of the Ppy inverse opal at oxidation (the green line) and neutral state (the orange line). The inset shows the conductivity switch of the sample at the two states.

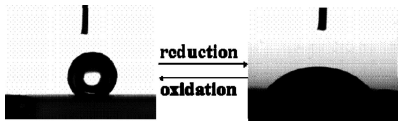

Figure 4. Water-drop profiles for as-prepared Ppy inverse opal, the water CA changed from 139.4° to 48.7° when being altered between oxidation (left) and neutral (right) state.

to neutral state. The increase of the sphere voids was mainly originated from the expension resulting from the insertion of Li^+,[11] the insertion of Li^+ also aroused the increase of refractive index of Ppy.[13d,15b] The increase of sphere voids and refractive index of ppy resulted in redshift of stopband for 50 nm in Figure 2a. Additionally, the volume of the neutral state could recover to the oxidation state (Figure 1c) after oxidation procedure, which led to the contraction of the film accompanying the decrease of refractive index.[13d,15b] Thus, the tuning of both the volume and the refractive index caused the reversible modulation of the stopband position in Figure 2b. It should be noted that there was a tiny increase of the reflectance intensity at neutral state comparing with that of the oxidation state. This enhanced optical signal at neutral state could be ascribed to the more ordered structure due to the extension[2c,5a,6a] stemming from the Li^+ doping. This change could be clearly observed by comparing the SEM image of Figure 1c with that of Figure 1d.

Furthermore, the optical properties could be modulated step by step through varying the doping level of Li^+ as shown in Figure 2c. At the beginning of the reduction, there was a large red shift of stopbands because Li^+ doped into the Ppy film easily. Along with the reaction carrying out, the shift became smaller because the doping procedure became difficult. After reduction for 16 min, the concentration of Li^+ reached saturation in the Ppy film, and the stopband kept constant. Similar phenomena were observed during the oxidation procedure. The stopband position could gradually return to 576 nm after oxidation for 16 min.

On the other hand, the conductivity of the Ppy inverse opals showed a reversible transition between the two states accompanying with its color change. Figure 3 shows the $I-V$ curve of the Ppy inverse opals. Clearly, The conductivity was relatively high at the oxidation state, and the value was decreased by 4−5 times at the neutral state. In detail, the conductivity was approximately 5.2 S cm^{-1} at the oxidation state, and the value lowered to approximately 1.1 S cm^{-1} at the neutral state. Additionally, the conductivity of the Ppy inverse opals could be reversibly switched between the two states as shown in the inset of Figure 3. The reversible change of Ppy's conductivity was caused by the doping or dedoping of Li^+. At the neutral state, the doped Li^+ attracted the free electrons inside the Ppy polymer, which restricted the movement of the electron and resulted in the decrease of the conductivity of the film. In contrast, the deinsertion of Li^+ at the oxidation state would promote the movement of free electron and lead to the increase of conductivity. [10c,12]

Simultaneously, the wettablity of the Ppy inverse opal could be modulated reversibly as well. Figure 4 shows the water contact angle of the Ppy inverse opal at oxidation and neutral state, respectively. The value reversibly changed from 139.4° to 48.7° when dedoping or doping Li^+. The wettablility of the Ppy film strongly depends on the types of dopants used.[12,16] In our case, at the oxidation state, the film showed hydrophobicity due to the doping of DBS^- with a hydrophobic long alkyl chain.[12,16] In contrast, the film showed hydrophilicity at the neutral state due to the introduction of the hydrophilic Li^+. XPS data in Table S1, Supporting Information, revealed that little Li^+ dopant existed at the oxidation Ppy film but significant amounts were found at the neutral state. These results further confirmed the change of the surface chemical composition from hydrophobic to hydrophilic when varying from oxidation to neutral state. Otherwise, the roughness of the inverse opal structure also contributed to the enlargement of wettability change.[14b,c,17,18] Thus, the wettablity of the Ppy inverse opal changed from highly hydrophobic to highly hydrophilic when being altered between the oxidation and the neutral state.

In conclusion, high quaility Ppy (DBS) inverse opals were fabricated via PC template made from latex spheres with hydrophobic PS core and hydrophilic PMMA-PAA shell. The stopband of the material showed reversible conversion between the oxidation and the neutral state. Both the conductivity and the wettablitiy of the Ppy inverse opal could be switched accompanying with the color change. These multifunctional responses would endow the material promising applications in biosensors, optoelectronic devices, and microfluidic devices.

Acknowledgment. The authors thank Prof. Y.F. Li for the helpful discussion and are grateful for the support of the NSFC (Grants 50625312, 60601027, U0634004, and 20721061) and the 973 Program (Nos. 2006CB806200, 2006CB932100, 2006 CB921706, and 2007CB936403). The Chinese Academy of Sciences is gratefully acknowledged.

Supporting Information Available: Experiemntal details and SEM images, cyclic voltammograms, and XPS results. This material is available free of charge via the Internet at http://pubs.acs.org.

CM800444A

(15) (a) Park, S. H.; Xia, Y. *Langmuir* **1999**, *15*, 266. (b) Yoshino, K.; Satoh, S.; Shimoda, Y.; Kawagishi, Y.; Nakayama, K.; Ozaki, M. *Jpn. J. Appl. Phys.* **1999**, *38*, L961.
(16) (a) Mecerreyes, D.; Alvaro, V.; Cantero, I.; Bengoetxea, M.; Calvo, P. A.; Grande, H.; Rodriguez, J.; Pomposo, J. A. *Adv. Mater.* **2002**, *14*, 749. (b) Azioune, A.; Chehimi, M. M.; Miksa, B.; Basinska, T.; Slomkowski, S. *Langmuir* **2002**, *18*, 1150.
(17) (a) Gu, Z-Z.; Uetsuka, H.; Takahashi, K.; Nakajima, R.; Onishi, H.; Fujishima, A.; Sato, O. *Angew. Chem., Int. Ed.* **2003**, *42*, 894. (b) Shiu, J. Y.; Kuo, C. W.; Chen, P. L.; Mou, C. Y. *Chem. Mater.* **2004**, *16*, 561.
(18) (a) Sun, T.; Feng, L.; Gao, X.; Jiang, L. *Acc. Chem. Res.* **2005**, *38*, 644. (b) Martines, E.; Seunarine, K.; Morgan, H.; Gadegaard, N.; Wilkinson, C. D. W.; Riehle, M. O. *Nano Lett.* **2005**, *5*, 2097.